Available online at www.sciencedirect.com
SCIENCE DIRECT®
Scripta Materialia 53 (2005) 201–206
Scripta MATERIALIA
www.actamat-journals.com

Effects of friction stir processing on mechanical properties of the cast aluminum alloys A319 and A356 ☆

M.L. Santella [a,*], T. Engstrom [b], D. Storjohann [b], T.-Y. Pan [c]

[a] *Metals and Ceramics Division, Oak Ridge National Laboratory, Oak Ridge, TN 37831-6096, USA*
[b] *Materials and Metallurgical Engineering Department, South Dakota School of Mines and Technology, Rapid City, SD 57701, USA*
[c] *Scientific Research Laboratories, Ford Motor Company, 2101 Village Road, Dearborn, MI 48124, USA*

Received 19 March 2005; received in revised form 19 March 2005; accepted 23 March 2005
Available online 18 April 2005

Abstract

Surfaces of A319 and A356 castings were treated by friction stir processing to reduce porosity and to create more uniform distributions of second-phase particles. Dendritic microstructures were eliminated in stir zones. The ultimate tensile strengths, ductilities, and fatigue lives of both alloys were increased by the friction stir processing.

Keywords: Aluminum alloys; Casting; Friction stir welding; Mechanical properties; Surface structure

1. Introduction

The use of the friction stir process primarily to modify microstructures is not as well developed as it is for welding, but its potential is becoming apparent. Friction stir welding creates bonds through the combined effects of heat, deformation by a stirring action, and pressure using a nonconsumable tool that is translated along a joint line [1]. While it uses the same type of equipment and procedures, bonding materials together is not the objective of friction stir processing. Instead, friction stir processing is a means to locally modify properties over depths or volumes that depend on the material being processed and the desired effect. Friction stir processing can dramatically refine grain structures producing improvements in a variety of properties [2–5]. Some examples include conditioning microstructures of wrought Al alloys for high strain rate superplastic deformation [3], and refining microstructures to improve ductility of high-strength powder metallurgy Al nanocomposite alloys [4]. Other innovative applications are for improving the cold-workability of wrought Al plate [6], and improving the mechanical properties of both Al castings [7–9] and fusion welds of wrought Al plate [10,11].

The objective of the present work was also to evaluate the extent to which friction stir processing could improve local mechanical properties of Al castings. Two cast alloys were used, A356 and A319. These were chosen because they are important for many automotive components, such as suspension, driveline, and engine parts, where increased durability and reliability are always desirable.

2. Experimental details

The specimens used for the friction stir processing experiments were machined from sand-cast ingots into

☆ This manuscript has been authored by a contractor of the US Government under contract DEAC05-00OR22725. Accordingly, the US Government retains a nonexclusive, royalty-free license to publish or reproduce the published form of the contribution, or allow others to do so for US Government purposes.

* Corresponding author. Tel.: +1 423 574 4805; fax: +1 423 574 4928.
E-mail address: santellaml@ornl.gov (M.L. Santella).

1359-6462/$ - see front matter © 2005 Acta Materialia Inc. Published by Elsevier Ltd. All rights reserved.
doi:10.1016/j.scriptamat.2005.03.040

16 mm × 50 mm × 200 mm bars. Two alloys were used: A356 (nominally Al–7Si–0.3Mg, wt.%) and A319 (nominally, Al–6Si–3.5Cu, wt.%).

The friction stir processing was done on a milling machine with the position of the stir tool fixed relative to the surface of the bars. The tool was made of H13 steel with a shoulder diameter of 13 mm. The pin was cylindrical with a hemispherical tip; its dimensions were 5.2 mm diameter × 3.4 mm length. The working surfaces of the stir tool were smooth. The tool rotation speed was set at 1000 rpm, and the translation speed fixed at 1.7 mm/s throughout the experiments. These conditions were used to make stir passes with lengths of about 150 mm. Some testing and analysis was done using single stir passes. Other bars were processed with 5–6 passes overlapped on intervals of about 4 mm. Overlapping the passes created relatively consistent stir processed volumes on the bars with dimensions of about 3 mm × 20 mm × 150 mm.

The room temperature properties of the friction stir processed bars were measured by Vickers microhardness testing, tensile testing, and fatigue testing. The microhardness measurements were made on metallographically prepared specimens taken to view the surfaces of single stir passes. The indentations were made under a 50 g load in 200 μm × 200 μm arrays extending from the stir zones into the base metal.

The bars with the overlapped passes were used to make both tensile and fatigue test specimens. For the tensile specimens, blanks were electrical discharge machined (EDM) across the stir zones, i.e., transverse to the translation direction. Slices 2-mm thick were then EDM cut from both surfaces of the blanks to provide one specimen of base metal and one specimen where the gage section was entirely within the friction stir processed material. The gage length and width dimensions were 12.5 mm and 3 mm, respectively. The nominal strain rate for the tensile tests was 1×10^{-3}/s.

Fatigue test specimens were prepared using a similar approach except that because longer specimens were required their axes were oriented in the translation direction. The specimens were a type having gage sections with tangentially blended fillets. The minimum dimensions in the test section were 6.4 mm wide × 2 mm thick. To avoid buckling, two specimens were glued together with a thin layer of slow cure epoxy.

Metallographic examinations were done on unetched specimens only.

3. Results

The microstructures of the two cast alloys are shown in Fig. 1. Both consist of primary Al alloy dendrites with interdendritic regions of Al intermetallic phases and elemental Si [12]. Both also contain relatively large primary

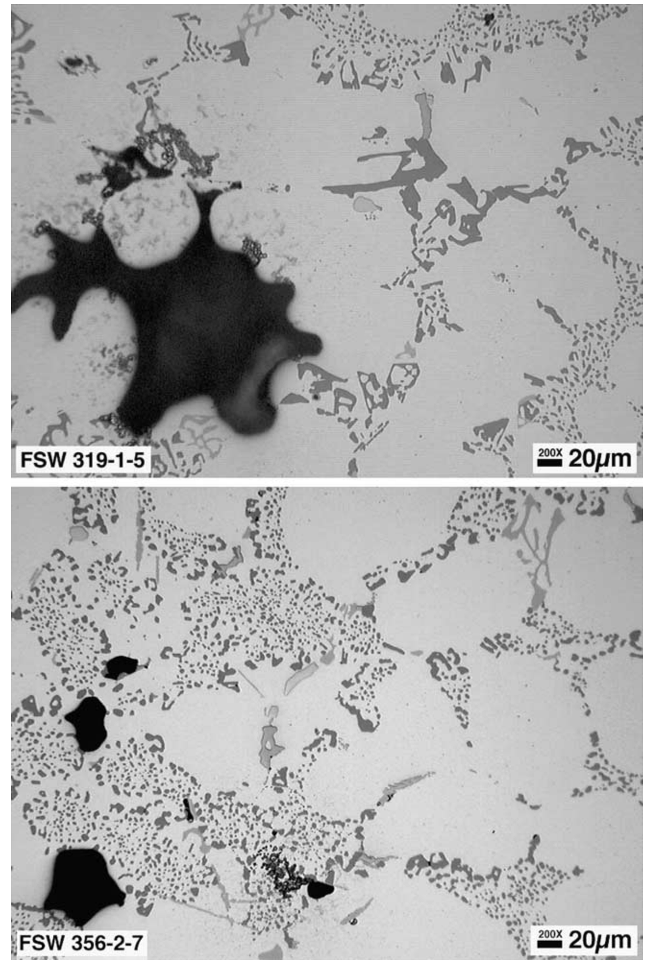

Fig. 1. Optical micrographs showing as-cast microstructures of A319 (top) and A356 (bottom) sand castings.

intermetallic particles and shrinkage porosity. The effect of friction stir processing on these microstructures is illustrated in Fig. 2. The microstructure at the boundary of the stir zone and the A319 base metal is shown in Fig. 2(a); that near the center of the stir zone is shown in Fig. 2(b). The stirring action closed porosity, fractured large second-phase particles reducing both their average size and aspect ratios, and uniformly distributed particles throughout the stir zone microstructure. Virtually all traces of dendritic solidification microstructure were eliminated throughout the stir zones. Identical behavior was found for A356 as others have observed [7–9].

The effect of friction stir processing on the distribution of hardness on the A319 surface is illustrated by Fig. 3. Soft spots found in the casting due to porosity and Al dendrite cores were eliminated by the friction stir processing. The distribution of hardness values also appears narrower in the stir zone. This is consistent with its more uniform microstructure. For A319, average microhardness values were 709 ± 166 MPa over 300 indents in the casting, and 802 ± 89 MPa over 200 indents in the stir zone. The general features of hardness distri-

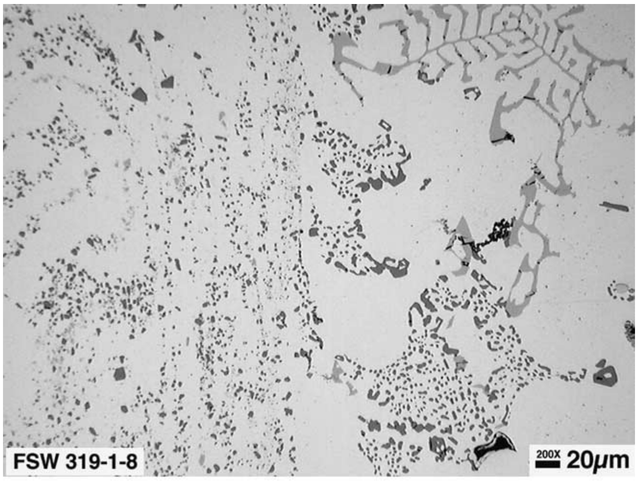

(a)

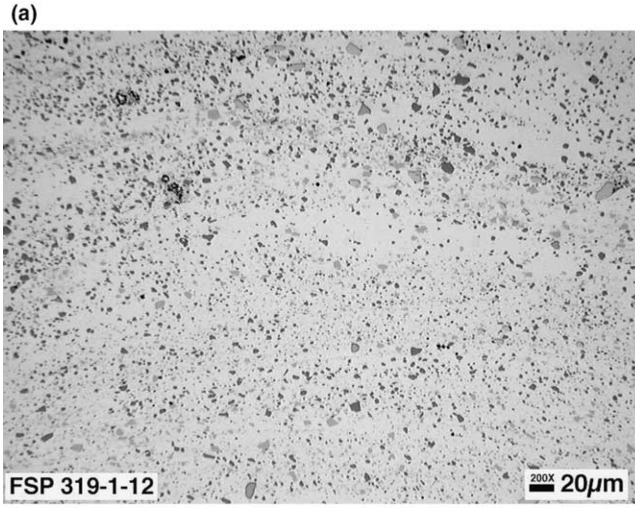

(b)

Fig. 2. Optical micrographs showing (a) the boundary between A319 cast base metal on right and the friction stir processed zone on left and (b) a region near center of the stir zone.

bution for A356 were virtually identical to those of A319. However, the average hardness values of the A356 casting and stir zone were 583 ± 60 MPa and 522 ± 32 MPa, respectively. These results show that the thermomechanical treatment cycle of the friction stir processing had a hardening effect in A319 and a slight softening effect in A356. Others have also found that the hardness of friction stir processed A356 is similar to that of the cast metal [7].

Data comparing the tensile behavior of cast and friction stir processed metal are presented in Fig. 4 and Table 1. Both alloys experienced large ductility increases for friction processed material. The markers in Fig. 4(a) indicate the fracture strains for the A319 specimens which all failed with no significant necking. Friction stir processing of this alloy increased the maximum total elongations from under 1% to over 7%. The yield points of the friction stir processed specimens were also slightly higher than those measured for the cast metal which is consistent with the hardness measurements. In contrast, the A356 specimens did display necking before failure. Friction stir processing increased total uniform elongation values in this alloy from under 3% to over 12%. The stir processed A356 had slightly lower yield strength than the cast metal as the hardness data would indicate. It should be noted that the cast bars were heated by the friction stir processing. As a consequence, the cast specimens of both alloys were subjected to multiple undefined thermal excursions. These unintended heat treatments could influence property values of the casting [13,14]. However, the stir processed material would have been subjected to similar heat treatments so that the comparison of tensile properties is still considered valid.

Because only one specimen in each condition was fatigue tested *S–N* curves could not be developed. Instead, specimens were tested at 138 MPa to directly compare the as-cast and friction stir processed alloys. These results are given in Table 2. The fatigue tests were fully reversed. The strain amplitudes were selected based on experience and with the intention of producing similar loading conditions in both the A356 and the A319 specimens. However, the A319 specimens maintained a pronounced mean stress even though their hysteresis loops were elastic. A consequence of this behavior was that different strain amplitudes were used for the two alloys. For both alloys, the friction stir processed specimen had significant extended life compared to the as-cast condition.

4. Discussion

Metallographic examinations indicate that friction stir processing is equally effective for refining microstructures in A356 and A319. The break up of large irregularly shaped Si and intermetallic particles attests to the severe deformations caused by the friction stirring action. The effect of reducing the aspect ratio of Si particles is similar to that of using Sr to modify melts prior to casting [13,15,16]. However, in terms of microstructures, friction stir processing has the added benefits that particles are more uniformly distributed than in cast structures, and that other intermetallic phases are also reduced in size and aspect ratio. The uniformity of stir zone microstructures as viewed from the original cast bar surfaces further indicates that stir tools of simple shapes and surface details are effective for deriving significant benefits from the friction stir processing. The stir zones were not subjected to analysis of porosity, but optically visible porosity was significantly reduced and solidification substructure eliminated. The reduction of porosity was also at least partly responsible for the elimination of microstructural soft spots indicated in the stir zones by hardness testing. Clearly, much more extensive analyses are needed to determine the effects of

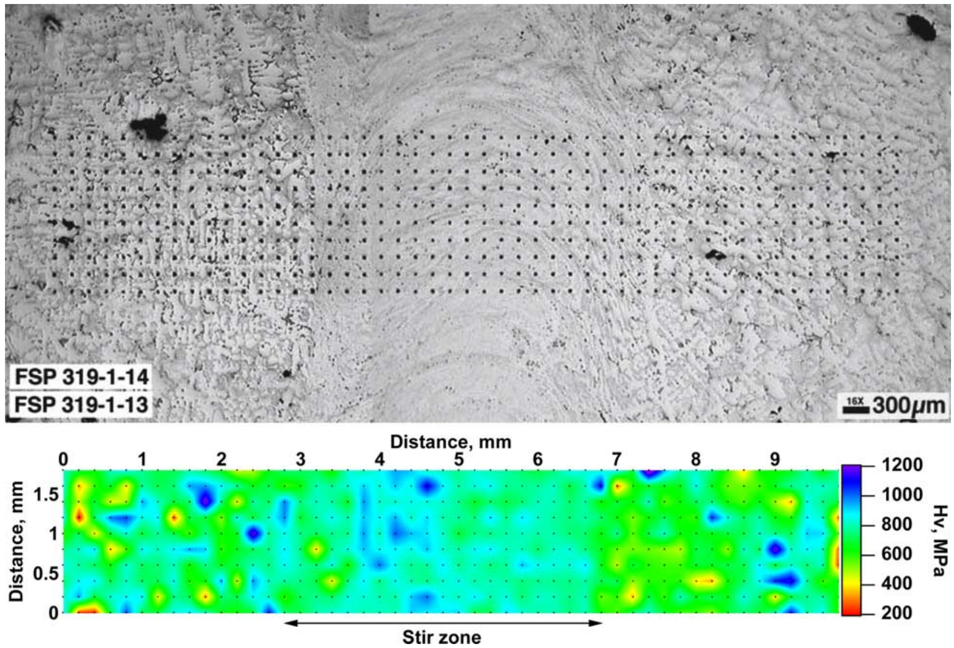

Fig. 3. Optical micrograph showing top view of a friction stir pass on the surface of an A319 cast bar. Microhardness distribution is shown on the bottom.

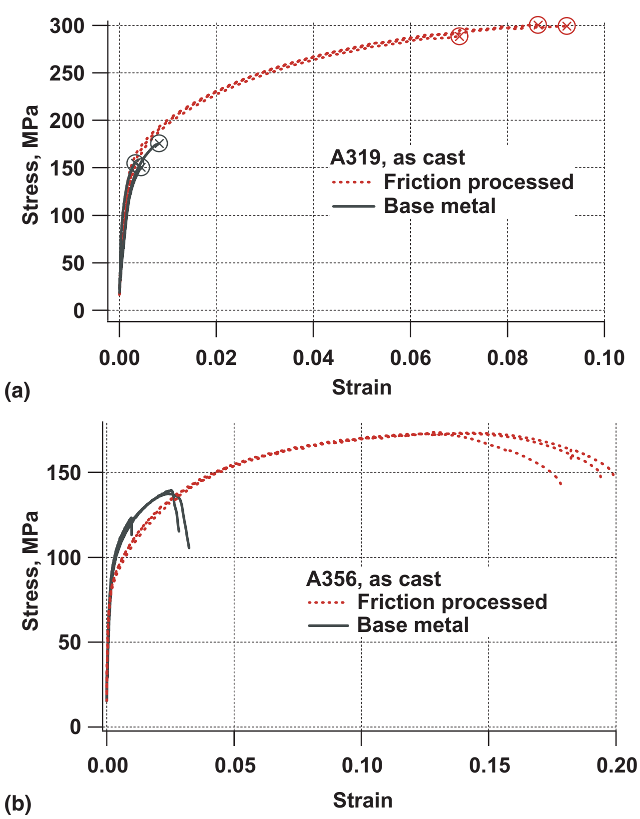

Fig. 4. Stress–strain plots from room temperature tensile tests done on cast and friction stir processed A319 (a) and A356 (b).

friction stir processing on the microstructures of these alloys.

Table 1
Comparison of tensile properties for cast and friction stir processed (FSP) A356 and A319

Condition	0.2% Yield strength (MPa)	Tensile strength (MPa)	Uniform elongation (%)
Cast A319	–	154.8	0.5
	151.5	151.5	0.5
	157.2	175.6	0.9
FSP A319	163.6	300.2	8.5
	167.6	300.4	8.6
	157.5	288.3	7.0
Cast A356	99.1	139.5	2.5
	100.2	137.4	2.4
	101.8	123.2	1.2
FSP A356	86.7	173.6	12.8
	88.2	172.8	13.9
	86.5	172.6	12.4

Table 2
Comparison of fatigue life for cast and friction stir processed (FSP) A356 and A319

Condition	Strain amplitude	Stress (MPa) amplitude at half-life	Number of cycles to failure
As-cast 356	0.002	108	7700
FSP 356	0.002	136	93,848
As-cast 319	0.0014	93.6	100,980
FSP 319	0.0014	126	281,442

Handbook values of yield strengths for sand cast A319 and A356 (F or T1 temper) are near 124 MPa and 83 MPa, respectively [13,17]. The tensile behaviors illustrated by Fig. 4 and shown in Table 1 for both the cast A319 and A356 deviate somewhat from the typical ranges. This could be the result of unintended heat treatments during the friction stir processing, or it could be due to the effects of casting conditions, porosity, or composition [15,16,18]. However, a detailed analysis of how various materials and processing parameters influence the tensile behavior of A319 and A356 castings is beyond the scope of the present experiments.

The most striking features illustrated by Fig. 4 and Table 1 are the large ductility increases produced in both alloys by friction stir processing. The improved ductilities were accompanied by increases in ultimate tensile strengths as well. The trend of increasing tensile strength being associated with increased ductility is typical of cast A319 [16]. For the friction stir processed A319, the tensile strength and ductility are on the order of those found in chill castings that were subsequently heat treated to the T6 condition [16]. For heat treated A356, strength increases are usually associated with reduced tensile elongations [13]. In contrast, these tensile properties are simultaneously increased in A356 by friction stir processing.

The tensile properties of A319 and A356 are strongly dependent on porosity levels, scale of the microstructures, and heat treatments [13–16], and the independent effects of a single variable may be difficult to isolate. However, ultimate tensile strengths and ductilities generally improve as porosity levels and microstructure scale decrease. The tensile behavior of the friction stir processed A356 and A319 are consistent with this behavior pattern.

The fatigue properties of Al castings depend on not only porosity and second-phase particles, but on their sizes, shapes, and distributions in microstructures [18–20]. For a particular size, defects that are closer to a surface are much more potent fatigue failure initiation sites than ones in specimen interiors [18,19]. The procedure of cementing specimens together that was used to measure the data shown in Table 1 effectively doubles the effects of near surface defects on fatigue properties. This also makes it difficult to directly compare these properties with other published data from monolithic specimens of the same size and shape. Nevertheless, the results in Table 1 represent an internally consistent data set that is also generally consistent with the microstructure modifications produced by friction stir processing. The friction stir processed specimens of both A356 and A319 had reduced porosity and more uniformly sized and distributed second-phase particles of aspect ratio near 1. These types of microstructure modifications would imply better fatigue properties as was observed.

All together, these initial results illustrate the potential of friction stir processing to improve the properties of both A356 and A319. The ability to apply friction stir processing to specific locations makes it a viable alternative to the hot isostatic pressing of entire castings. Because it can be accomplished on standard milling machines the incorporation of friction stir processing into machining procedures of certain components seems plausible.

5. Summary

Surfaces of bars cut from A319 and A356 castings were modified by friction stir processing. In contrast to the as-cast conditions, microstructures in the stir zones were characterized by relatively uniform distributions of second-phase particles that were also relatively uniform in shape. Visible porosity and dendritic microstructures were eliminated. Microhardness distributions were more uniform. The ultimate tensile strengths, ductilities, and fatigue lives of both alloys were increased by the friction stir processing.

Acknowledgments

Research sponsored by the US Department of Energy, Assistant Secretary for Energy Efficiency and Renewable Energy, Office of FreedomCAR and Vehicle Technologies, as part of the High Strength Weight Reduction Materials Program (VT0502020/VT0602010, CEVT023), under contract DE-AC05-00OR22725 with UT-Battelle, LLC. Technical reviews and comments by S. S. Babu and Q. Han are appreciated. The authors are also grateful to F. A. Conle and A. R. Krause for assistance with the fatigue testing, and to J. M. Boileau and J. E. Allison for their technical support and guidance regarding the casting and properties of aluminum alloys.

References

[1] Dawes CJ. Weld Met Fab 1995;63:13–4.

[2] Mishra RS, Mahoney MW, McFadden SX, Mara NA, Mukherjee AK. Scripta Mater 2000;42:163–8.

[3] Berbon PB, Bingel WH, Mishra RS, Bampton CC, Mahoney MW. Scripta Mater 2001;44:61–6.

[4] Saito N, Shigematsu I, Komaya T, Tamaki T, Yamauchi G, Nakamura M. J Mater Sci Lett 2001;20:1913–5.

[5] Mahoney MW, Binget WH, Mishra RS. Mater Sci Forum 2003;426:2843–8.

[6] Vaze SP, Xu J, Ritter RJ, Colligan KJ, Fisher Jr JJ, Pickens JR. Mater Sci Forum 2003;426–432:2979–86.

[7] Lee WB, Lee YM, Jung SB. Mater Sci Eng 2003;A355:154–9.

[8] Ma ZY, Sharma SR, Mishra RS, Mahoney MW. Mater Sci Forum 2003;426:2891–6.

[9] Sharma SR, Ma ZY, Mishra RS. Scripta Mater 2004;51:237–41.

[10] Fuller C, Mahoney M, Bingel W. Friction stir processing of aluminum fusion alloys. In: Proceedings of the 4th international friction stir welding symposium, TWI, Abington; 2003.

[11] Mahoney MW, Lynch SP. Friction stir processing. In: Paper 23 in proceedings, surface engineering conference. Welding Technology Institute of Australia, Silverwater, NSW; 2003.
[12] Solidification characteristics of aluminum alloys. In: Backerud L, Chai G, Tamminen J, editors. Vol. 2: Foundry Alloys. Schaumburg, IL: American Foundry Society; 1990.
[13] Apelian D, Shivkumar S, Sigworth G. Am Found Soc Trans 1989;89–137:727–42.
[14] Kashyap KT, Murali S, Raman KS, Murthy KSS. Mater Sci Technol 1993;9:189–203.
[15] Closset B, Gruzleski J Metall Trans 1982;13A:945–51.
[16] Li Z, Samuel AM, Samuel FH, Ravindran C, Valtierra S, Doty HW. Mater. Sci. Eng. 2004;A367:96–110.
[17] Metals handbook desk edition. 2nd ed. Metals Park, OH: ASM International; 1998.
[18] Seniw ME, Conley JG, Fine ME. Mater Sci Eng 2000; A285:43–8.
[19] Atxaga G, Pelayo A, Irisarri AM. Mater Sci Technol 2001;17:446–50.
[20] Boileau JM, Allison JE. Metall. Mater Trans 2003;34A:1807–20.